JOURNAL OF CATALYSIS 121, 356–363 (1990)

Size Distributions of Supported Metal Catalysts: An Analytical X-Ray Line Profile Fitting Routine

W. VOGEL

Fritz-Haber-Institut der Max-Planck-Gesellschaft, Faradayweg 4-6, 1000 Berlin 33, West Germany

Received August 31, 1988; revised September 19, 1989

Two simple analytical functions containing a single structural parameter are derived by consideration of boundary conditions for the so-called "column length distribution" of crystallites. Assuming spherically shaped crystallites the distribution functions of the diameters are derived. The type I distribution includes "atomic" dispersion while type II corresponds to a minimum crystallite size. The use of such functions, rather than the application of the Warren–Averbach analysis to X-ray line profiles, is shown to be favoured in the case of highly dispersed and unstrained supported metal catalysts. These functions fit the line profiles of a series of Pt/SiO_2 catalysts extremely well. For these catalysts the type I distribution gives the best fit at low dispersion levels d_H of 6 and 21%, whereas for $d_H = 40\%$ crystallite dispersion of type II seems normal. Additionally the related X-ray dispersions d_X have good correlation with the hydrogen chemisorption values d_H.

INTRODUCTION

In treating X-ray diffraction data obtained from metal crystallites, Houska and Smith (*1*) first introduced analytical functions assuming spherical particles, nonuniform strains, and instrumental broadening rather than applying the classical Warren–Averbach analysis (*2*) to the X-ray diffraction profiles. The former approach gives useful results even though the entire profile is not available. Later Rao and Houska (*3*) extended the single-size-sphere model to include a variation in sphere size. This type of treatment is of great use for bulk polycrystalline materials which in general are strained by dislocations and grain boundaries.

This paper describes a simplified approach which applies to the case of isolated, undisturbed small metal crystallites, where the contribution of strain and instrumental broadening may be neglected. This situation is found in highly dispersed supported metal catalysts, which have been given a suitable standard pretreatment. The diffraction profiles are then simply governed by the crystallite size distribution. It has been shown from the early work of Bertaut (*4*) that the second derivative of the Fourier transformed profile (column length distribution) equals the distribution of the diameters normal to the reflecting net planes, collected over the cross sections of all crystallites.

We assume the interaction of the metal with the support (substrate) to be weak; i.e., there should be no strong geometrical correlation between atoms at the metal–substrate interface. Thus the interference terms of the two phases should cancel out. Interference effects will be strongly diminished if the difference in atomic number of the metal versus substrate is large. A Debye function model calculation shows that the intensity of a 32-atom Pt cluster is altered by less than 2% if its (001) surface approaches the oxygen atoms in the (001) surface plane of β-christobalite, going down from large distances to the usual Pt–O bond length of 2.1 Å.

Due to the low metal loading of the order of 1 wt%, or less, the metal reflections are strongly masked by the support scattering. Consequently, line profiles are available over a limited range and with a limited

0021-9517/90 $3.00

knowledge of the true baseline. The numerical treatment according to the general relation outlined above will fail due to the lack of this information.

In the following sections we will apply a simple analytical distribution function with the proper asymptotical behavior to fit the measured diffraction profiles. Allowance is given for a weighted average of such functions to improve the profile fit and to retain a more general solution. This solution will be compared with the results of the standard Fourier analysis and will be discussed in several practical examples.

THEORY

Let $A(x)$ be the Fourier transform of an X-ray line profile, where $x = r/L$ is a dimensionless positive variable related to the distance r in physical space and L, an arbitrarily defined length. According to Ref. (*2*) the general bounding conditions of the column length distribution $A''(x)$, which must be obeyed for the second derivative of $A(x)$, are

$$A''(x) \geqq 0 \text{ for all } x;$$
$$A''(x) \to 0 \text{ for } x \to 0 \text{ and } x \to \infty. \quad (1)$$

The simplest functions obeying these rules are

$$A(x) = P(x)e^{-x}, \quad (2)$$

where $P(x) = a_0 + a_1x + a_2x^2 + \ldots$, with

$$\text{I.} \quad a_0 = 1;\ a_1 = \tfrac{1}{2} \quad (3)$$

$$\text{II.} \quad a_0 = 1;\ a_1 = \tfrac{7}{10};\ a_2 = \tfrac{1}{5};\ a_3 = \tfrac{1}{40}. \quad (4)$$

Taking $a_0 = 1$ for convenience, it follows from $A''(0) = 0$ that $a_1 = \frac{1}{2}$ for solution I. Using the abbreviation $B(x) = A''(x)/x$ the coefficients of solution II are obtained by the additional conditions $B'(0) = 0$ and $B''(0) = 0$.

The average crystallite size l from Fourier line profile analysis is $l = -A(0)/(A'(r))_{r=0}$, which is $l = 2L$ for solution I. According to Matyi *et al.* (*13*) this quantity is the surface average of the distribution. In catalysis, however, it is of interest to know the surface distribution versus the crystallite radii. To perform the step from the distribution of column length to the number distribution of sizes $H(D)$, a specific crystallite shape must be assumed. This will conveniently be chosen to be spherical, where D is the sphere diameter.

In the case of spheres $H(D)$ is related to $A(x)$ by

$$H(D) \propto d/dr(A''(r)/r)_{r=D}. \quad (5)$$

It is clear that the two types of functions represented by the coefficients in Eqs. (3) and (4) differ in a fundamental manner. For type I, $H(D)$ peaks at $D = 0$, while for type II $H(D) = 0$ for $D \to 0$. Hence for type I, atomic dispersion is included, while type II defines a minimum crystallite size. Since such atomically dispersed states are frequently discussed in catalyst literature, the differentiation between the two types of distributions appears to be important.

It can be easily shown that the fraction of single atoms to the total mass is negligible. However, metal clusters Me_n with $n \geqq 2$ give rise to a curved background around the Bragg nodes and contribute intensity to the wings of the Bragg peaks. Atomic dispersion, in this sense, means clusters with less than ~13 atoms, which in fact have all the atoms exposed to the surface.

The inverse Fourier transform of Eq. (2) leads to the analytical functions $f(b)$ used to fit the experimental line profile

$$f(b) = 2L \sum k!a_k \text{REAL}(u^{-k-1}); \quad u = 1 - i2\pi bL, \quad (6)$$

where $b = 2\sin(\theta)/\lambda$ is the distance in reciprocal space, θ is the Bragg angle, and λ is the wavelength. For type I distributions, Eq. (6) reduces to a Lorenzian plus a squared Lorenzian:

$$f(b) = (1 + 4\pi^2L^2b^2)^{-1} + 2(1 + 4\pi^2L^2b^2)^{-2}. \quad (7)$$

A sum of weighted functions $f(b)$ will be used to fit the line profile $i(b)$, the number

of terms being determined by possible improvements of the fit:

$$i(b) = \Sigma\, \alpha_j f_j(b); \quad \alpha_j = \text{weight fractions.} \tag{8}$$

According to Eq. (5) and with the abbreviation $x_j = D/L_j$ one obtains

$$H(D) \propto \Sigma\, (\alpha_j/L_j^4) x_j^m \exp(-x_j), \tag{9}$$

with $m = 0$ and 2 for types I and II, respectively.

The nth moment of the diameter distribution Eq. (9) is

$$\overline{D^n} = (n + m)!\, \Sigma\, \alpha_j L_j^{n-3}. \tag{10}$$

For two terms, for instance, the distribution function $H(D)$ is described by the three parameters α, L_1, and L_2. The distribution of the crystallite surface $S(D)$ and the crystallite mass $M(D)$ versus the sphere diameters is obtained by the products

$$S(D) \propto D^2 H(D); \quad M(D) \propto D^3 H(D). \tag{11}$$

$D_S = \overline{D^3}/\overline{D^2}$ and $D_M = \overline{D^4}/\overline{D^3}$ are the respective surface mean and mass mean diameters and can be evaluated from Eq. (10).

The polydispersity P as defined in Ref. (10) is a quantity related to the width of the distribution function. For the polydispersity of, for instance, the mass distribution we have

$$P_M = ((\overline{D^5}/\overline{D^3})/(\overline{D^4}/\overline{D^3})^2 - 1)^{1/2}. \tag{12}$$

For the numerical treatment a least-squares fit of nonlinear parameters by Marquardt (5) is well suited. The Pt diffraction profiles are obtained by subtracting the scattering of the pure substrate over a restricted range. A linear background is added to the fit-function (8) to correct for errors in the baseline position.

EXPERIMENTAL

The X-ray spectra were recorded by a commercial Guinier powder diffractometer (Huber) with a modified *in situ* specimen cell. The focusing Johansson-type germanium monochromator gives an intense Cu$K\alpha_1$ primary beam. Instrumental broadening of catalyst specimens can, in general, be neglected, due to high angular resolution ($\leqq 0.025°$) of the Guinier diffractometer.

TABLE 1

Structural Parameters of Catalyst No. 88 from Integral Linewidth Measurements

Treatment	Crystallite size (Å)	Internal strain (N/mm²)	Stacking faults (%)
Powder (untreated)	175	180	0.2
Pellet (untreated)	175	360	≦0.1
Pellet (300°C, H_2)	240	200	≦0.1
Pellet (500°C, H_2)	230	0	0.1

Note. After treatment at 500°C in H_2, the catalyst is fully recovered. For spherical crystallites, multiplication by $\frac{4}{3}$ should give the mass-averaged sphere diameter D_M; that is, $D_M = (\frac{4}{3})240 = 320$ Å compared to 354 Å in Table 2.

Four Pt/SiO_2 standard catalysts[1] prepared by Uchijima *et al.* (6) were investigated. The powder samples were pressed with 8000 kg to pellets 15 × 12 × 0.3 mm in size. Detailed characterisation of these catalysts has been given in Refs. (6–9).

RESULTS AND DISCUSSION

Figure 1 and Table 1 give the results of a linewidth analysis of catalyst No. 88 with a low Pt dispersion of ~6% (Ref. (6)) as a function of the treatment history. The integral linewidths δb of the first five platinum reflections are compared with the calculated linewidth by accounting for line broadening due to crystallite size, internal strains, and stacking faults (10, 11). The results indicate internal strains as high as 360 N/mm² for the untreated, pelleted sample, that is, twice the value of the untreated powder sample. The standard pretreatment at 300°C as described in Ref. (6) reduces the

[1] The relation of the code names used in Ref. (6) to the sample numbers used in the present text is: No. 88: 7.1-SiO_2–PtCl–S; No. 69: 21.5-SiO_2–Ion X–L; No. 65: 40-SiO_2–PtCl–L; and No. 67: 63.5-SiO_2–Ion X–L.

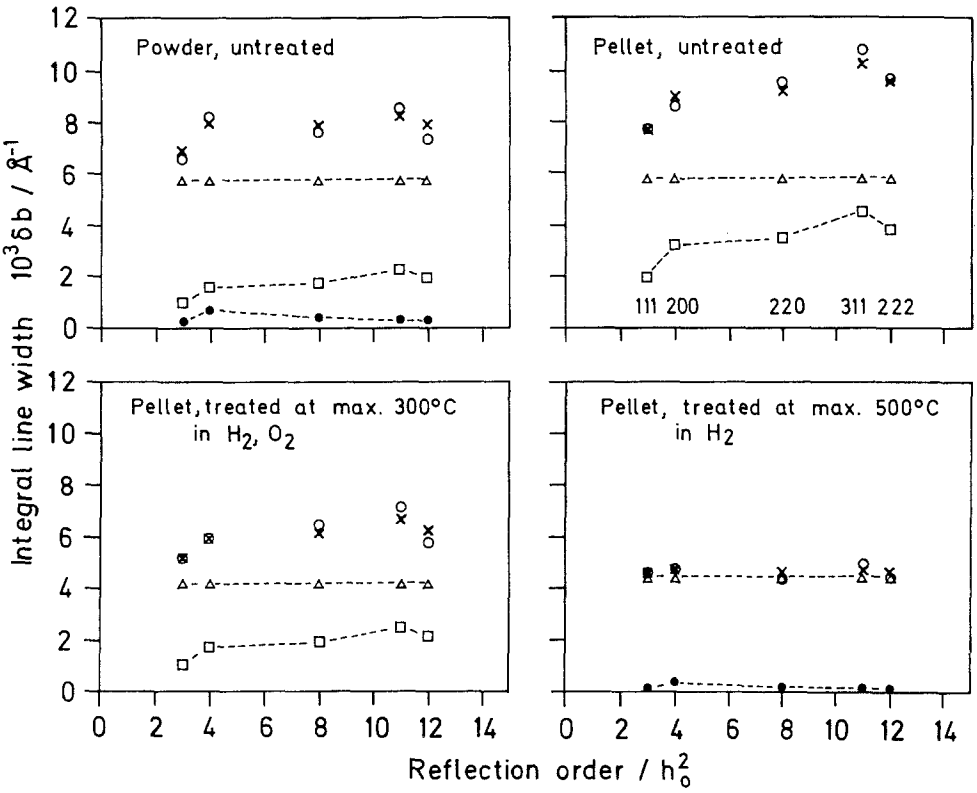

FIG. 1. The (111), (200), (220), (311), and (222) integral linewidth of catalyst 88 as a function of the reflection order h_0 and treatment history. Experimental (○) and theoretical (×); contribution of broadening due to size (△), internal strains (□), and stacking faults (●).

strain considerably and the mean crystallite size increases from 175 to 240 Å. Hydrogen treatment at 500°C leads to a complete recovery, but no more size increase. The increase in crystallite size is probably due either to a recrystallisation of the primary particles, which may be composed of subgrains, and/or to sintering.

High strains have already been reported by Nandi *et al.* (*9*) for a similar catalyst. However, they observed a decrease of crystallite sizes after hydrogen treatment at 450°C, together with an increased internal strain. The extremely long storage time of ~10 years in air might be the origin of these differences.

For catalyst No. 69 with a dispersion of 21% changes induced by pellet formation are much lower. Catalysts Nos. 65 and 67 with dispersions of 39.8 and 64.5%, respectively, did not show any induced changes. When hydrogen-treated at 500°C these catalysts are essentially defect free as observed from the linewidth. In a hydrogen atmosphere the interaction with the silica is lowest, as has been shown recently (*14, 15*). This justifies the application of the profile analysis outlined in the theoretical section.

Figures 2a and 2b show the (111) subtracted intensity of catalyst No. 69 (dots). The solid lines are the best fits using Eq. (8) including a single term, with a constant base line correction (dashed line). Figure 2a corresponds to a distribution including atomic dispersion, while Fig. 2b represents crystallite dispersion. Adding additional terms in Eq. (8) did not improve the *R*-factors ($R = \sqrt{\Delta^2 i / \bar{i}}$) of the fit ($R$ = 2.3 and 2.6%, respectively). The right-hand

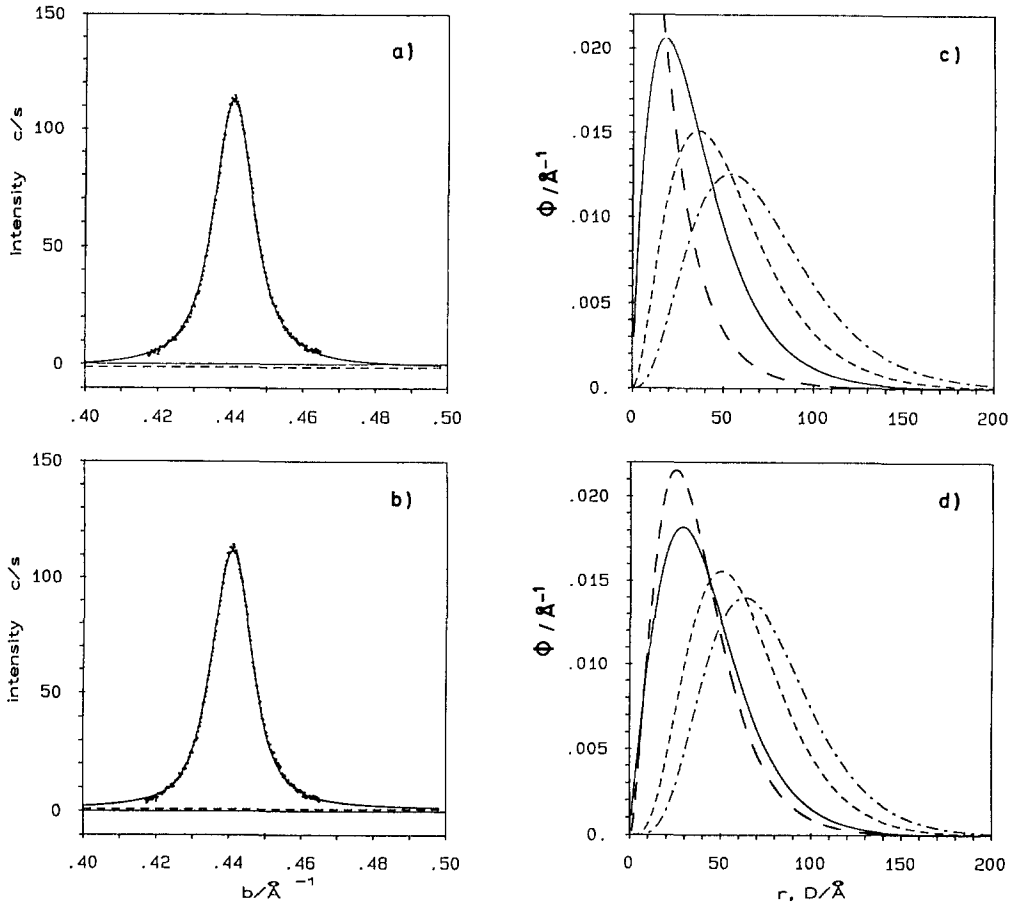

FIG. 2. The (111) line profile of catalyst 69 (dots) fitted by (a) one function type I; (b) one function type II (solid lines) plus a constant background (dashed lines); (c and d) are the corresponding distribution functions. The symbol Φ stands for four different normalized distribution functions: (1) distribution $A''(r)$ of columns with length r (solid line); (2) distribution $H(D)$ of number of spheres with diameter D (long dashed line); (3) distribution $S(D)$ of spheres, weighted by their surface (dashed line); (4) distribution $M(D)$ of spheres, weighted by their mass (dash-dotted line).

side of the figure shows the corresponding distribution functions as explained in the caption.

Although the distributions by number are very different, the corresponding distributions by mass are similar. This accounts for the fact that the powder line profiles are governed by the distribution of the masses of scattering crystallites. Thus the mass fraction of crystallites with diameters $D \leqq 0.3D_M$ is only 3.4 and 1% for distributions of type I and type II. For catalyst No. 69 $0.3D_M$ is approximately 20 Å.

The difference in the R-factors is too small to clearly favour a distribution of type I or type II. However, the quality of the fit proves that the proposed simple analytical distribution functions describe the state of dispersion of this catalyst adequately.

This is further established when we compare the column length distribution obtained with the usual Fourier analysis (Fig. 3). In this case, the tails of the (111) line profile were fitted to zero intensity by subjective judgment. As proposed by Pielaszek *et al.* (*12*) the Fourier coefficients were

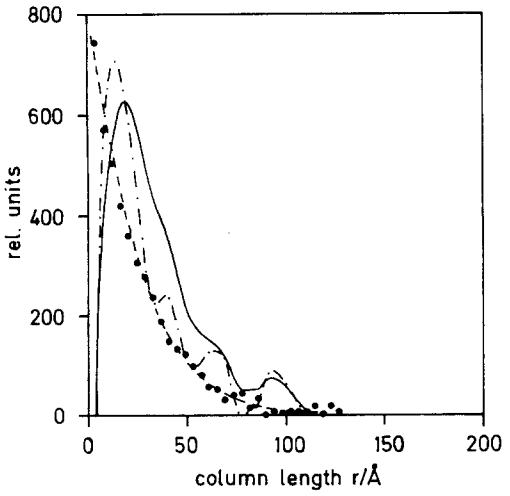

FIG. 3. Spline smooth (dashed line) of Fourier coefficients (●) from the (111) line profile of catalyst 69. The second derivative (solid line) gives the column length distribution. The latter is sensitive to the degree of smoothing. A reduced smoothing parameter gives the column length distribution shown by the dash-dotted curve.

spline smoothed before taking the second derivative. (Unfortunately there is no unique rule as to how to choose the involved smoothing parameter and the results depend strongly on this parameter, as shown by the dash-dotted curve in Fig. 3).

The Fourier analysis agrees with the column length distribution of Fig. 2c, that is with the atomic dispersion model. The direct determination of the size distribution of spheres from Fig. 3 according to Eq. (5) involves the third derivative and becomes completely uncertain, especially for small distances.

Catalyst No. 88, in the defect-free state, needs two terms in Eq. (8) for an improved line profile fit. Due to the larger crystallite sizes the tails of the (111) peak are known with more accuracy. The corresponding parameters of the fit, shown in Fig. 4a, are $\alpha_1 = 0.51$, $L_1 = 46.7$ Å, $\alpha_2 = 1 - \alpha_1$, and $L_2 = 133$ Å. The contributions of the two terms are separately plotted for the surface distribution in Fig. 4b. For catalyst No. 88 the distribution of type I is clearly favoured by the R-factor, as seen in Table 2.

Catalyst No. 65 with a nominal dispersion of 39.8% represents something like a limiting case for a meaningful X-ray line profile analysis. For even smaller crystallites the separation from the background scattering becomes doubtful. Comparison of the intensity over the total angular range covered by the experiment via Debye function calculations will then be superior to this method.

Figure 5a shows the fitted line profiles of the two overlapping (111) and (200) reflec-

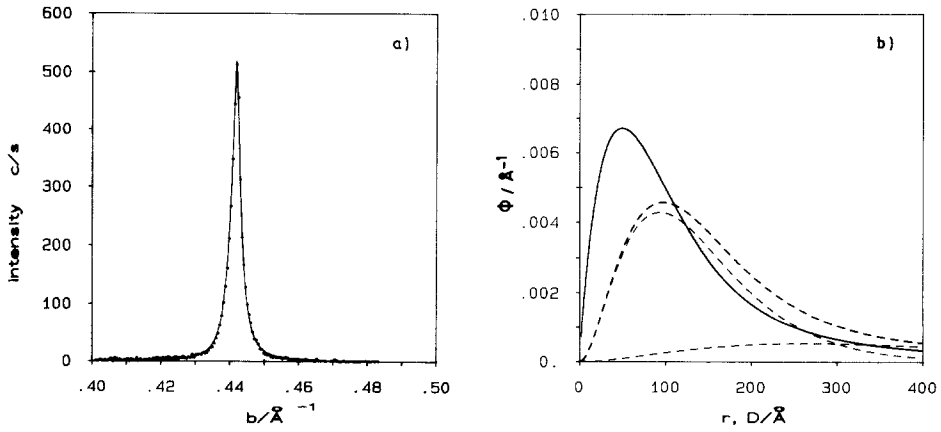

FIG. 4. (a) The (111) line profile of catalyst 88 (dots) fitted by two functions of type I. (b) Distribution $A''(r)$ of columns with length r (solid line). Surface-weighted distribution $S(D)$ of spheres with diameter D and the two terms contributing to $S(D)$ are indicated by dashed lines.

TABLE 2

X-Ray Results of the (111) Line Profile Analysis of Recovered Catalysts

Catalyst			X-ray results									
Pt			R-factor (%)		Ave. column length l (Å)		Ave. sphere diameters				X-ray dispersion d_X (%)	
							D_S (Å)		D_M (Å)			
No.	(wt%)	d_H (%)										
88	1.91	6.8	8.6	9.2	137	153	205	229	354	368	5.5	4.9
69	1.48	21.5	2.3	2.6	36	42	54	63	72	75	20.7	17.9
65	1.10	39.8	7.9	7.7	17	19	25	29	34	34	44.3	39.2
Distribution type			I	II	I	II	I	II	I	II	I	II

Note. The R-factors of the respective fits with functions of types I and II, average column length l, surface mean and mass mean sphere diameters D_S and D_M, and X-ray dispersion values $d_X = 11.2/D_S$ are given for three Pt/SiO_2 catalysts.

tions plus linear background. As in the case of catalyst No. 69, addition of a second term in Eq. (8) does not improve the fit. Within the limits of error the fit parameters are equal for the (111) and the (200) peaks. In contrast to the foregoing examples, catalyst No. 65 gives an improved fit by a type II distribution (Table 2). Figure 5b shows the corresponding distribution functions.

The outlined procedure is confined to size distributions with a lower limit of width. This limit is set by Eq. (12) to a minimum polydispersity $P_M = 50\%$, $P_H = 100\%$, and $P_M = 40\%$, $P_H = 58\%$ for the functions of type I and II, respectively. Clearly solutions to Eq. (1) with polynomials of higher order, which increase the exponent m in Eq. (9) and consequently lower the polydispersity, exist. For the sake of simplicity these have been confined to the most sim-

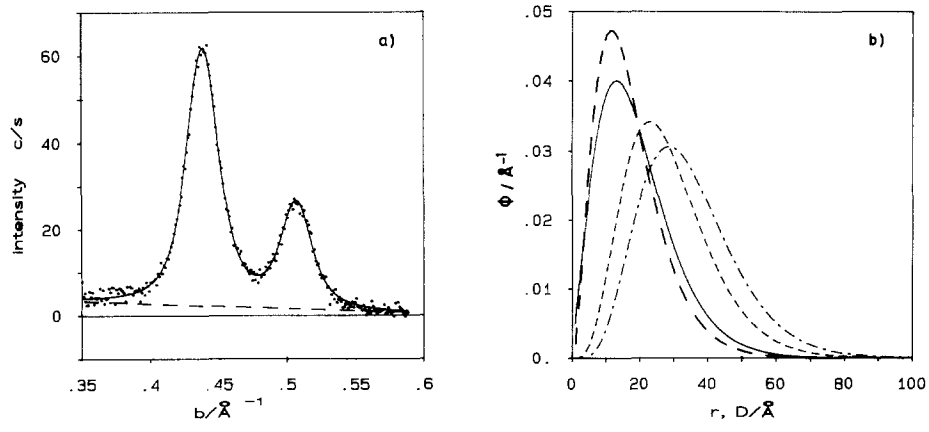

FIG. 5. (a) The (111)/(200) line profile of catalyst 65 (dots), each fitted by one function of type II (solid line) plus a linear background correction (dashed line). (b) The various distribution functions as explained in Fig. 2.

ple solutions that distinguish atomic dispersion. For the catalysts examined here the proposed functions are adequate.

REFERENCES

1. Houska, C. R., and Smith, T., *J. Appl. Phys.* **52,** 748 (1981).
2. Warren, B. E., "X-Ray Diffraction." Addison–Wesley, Reading, MA, 1969.
3. Rao, S., and Houska, C. R., *Acta Crystallogr. A* **42,** 14 (1986).
4. Bertaut, E. F., *Acta Crystallogr.* **3,** 14 (1950).
5. Marquardt, D. M., *J. Soc. Ind. Appl. Math.* **11,** 431 (1963).
6. Uchijima, T., Herrmann, J. M., Inoue, Y., Burwell, R. L., Jr., Butt, J. B., and Cohen, J. B., *J. Catal.* **50,** 464 (1977).
7. Sashital, R. S., Cohen, J. B., Burwell, R. L., Jr., and Butt, J. B., *J. Catal.* **50,** 479 (1977).
8. Otero-Schipper, P. H., Wachter, W. A., Butt, J. B., Burwell, R. L., Jr., and Cohen, J. B., *J. Catal.* **50,** 494 (1977).
9. Nandi, R. K., Molinaro, F., Tang, C., Cohen, J. B., Butt, J. B., and Burwell, R. L., Jr., *J. Catal.* **78,** 289 (1982).
10. Vogel, W., and Hosemann, R., *Z. Phys. Chem.* **121,** 193 (1980).
11. Vogel, W., Tesche, B., and Schulze, W., *Chem. Phys.* **74,** 137 (1983).
12. Pielaszek, J., Cohen, J. B., Burwell, R. L., Jr., and Butt, J. B., *J. Catal.* **80,** 479 (1983).
13. Matyi, R. J., Schwartz, L. J., and Butt, J. B., *Catal. Rev. Sci. Eng.* **29,** 41 (1987).
14. Gnutzmann, V., and Vogel, W., *Z. Phys. D* **12,** 597 (1989).
15. Gnutzmann, V., and Vogel, W., submitted for publication.